Automatic 3D Digital Dental Landmark Based on Point Transformation Weight

Sulaiman Triarjo
Department of Informatics
Institut Teknologi Sepuluh Nopember
Surabaya, Indonesia
6025211006@mhs.its.ac.id

Riyanarto Sarno*
Department of Informatics
Institut Teknologi Sepuluh Nopember
Surabaya, Indonesia
riyanarto@if.its.ac.id

Shintami Chusnul Hidayati
Department of Informatics
Institut Teknologi Sepuluh Nopember
Surabaya, Indonesia
shintami@if.ac.id

Gerry Sihaj
Department of Informatics
Institut Teknologi Sepuluh Nopember
Surabaya, Indonesia
gerrysihaj.19051@student.its.ac.id

2023 International Conference on Artificial Intelligence in Information and Communication (ICAIIC) | 978-1-6654-5645-6/23/$31.00 ©2023 IEEE | DOI: 10.1109/ICAIIC57133.2023.10067081

***Abstract*—Orthodontic treatment requires calculating the distance of specific points, or landmarks, of each tooth in a 3-dimensional (3D) arch model data. Orthodontic experts use an application to identify each tooth and point out the specific points in each tooth. Therefore, the dentition condition of the patient can be determined. This study proposed a new method to identify each tooth using deep learning combined with weighted mesh points. The deep learning method is used for the teeth segmentation process. The weighted mesh points method is used for determining the landmarks of each tooth automatically. The weighted mesh points method exploits the labelled mesh to calculate the suitable point to be a landmark. Deep learning is used to segment each tooth to set the type of tooth. Then, the weighted mesh of each tooth is calculated to set the landmarks. The algorithm successfully recognizes the specific points for each tooth with 2.225 in Root Mean Squared Error (RMSE).**

Keywords—Deep learning, Weighted, Tooth Landmark, Automation

I. Introduction

Many practitioners of dental health experts have already used the 3D dental image to process the patient data and decrease the usage of moulded wax [1]. It is used a scanner tool called an Intra-oral scanner [2]. It scans the teeth's surface with the gingiva while filtering the saliva [3]. The result is 3D data in the form of mesh which consist of a cloud of points and edges that connect one point to another to make triangle-shaped cells. It is different from 3D data in the form of voxel or DICOM, which format is being used by Magnetic Resonance Imaging. Voxel, or DICOM, consists of many layers of 2-dimensional images [4].

3D digital image processing has influenced the clinical practice in orthodontics. The analysis of jaws and dentition can be done in a 3D digital imaging application. Orthodontic experts analyze jaws and dentition by calculating the landmarks of each tooth. Determining the type of each tooth and identifying landmarks in each tooth can be time-consuming in a manual process [5].

Landmarks are specific points of a tooth used to calculate different analysis methods to determine a patient's dentition condition. Those are usually the mesial point and the distal point of a tooth [6][7][8][9]. In addition to those points, the ridge point, the cusp point, and the pit point are also searched [10][11][12][13]. Different type of tooth can have different set of landmarks. Therefore, it is essential to know what type of tooth it is first.

Detecting the type of tooth is challenging as the dentition condition of a patient can vary. Moreover, the form of the tooth varies, and a tooth of the same type can vary either. A person can have small teeth than average, and another can have bigger ones than average [14][15].

This paper proposed a pipeline method consisting of deep learning and mesh weighted that automatically finds landmarks in each tooth. This paper has a contribution that introduce weight in each point of tooth mesh to select a certain point as landmark. The experiment result shows that the proposed method can yield 3.258 in RMSE value.

The structure of this paper is organized as follows. Section II presents some related works, Section III describes the proposed method, and Section IV discusses the result of the experiment. Finally, Section V presents the conclusion and future work.

II. Related Work

The algorithm to segment each tooth in jaw is important to identify each tooth type. After each tooth type is acquired, the algorithm to find landmarks in each tooth takes place.

A. Tooth Segmentation

In recent studies in tooth segmentation, the researcher has used deep learning architectures. Zhang et al. [16] used Convolution Neural Networks (CNN) architecture in harmony parameter. The architecture in the study was based on the U-net network structure. The study yielded 98.87% in accuracy and 0.046 mm in Directional Cut Discrepancy (DCD). Later, Zanjani et al. [17] developed Mask-MCNet based on a deep neural network to segment teeth in 3D points clouds. It was a modified version of PointCNN. The method predicted a 3D bounding box of the tooth and segmented the points simultaneously. It achieved 98% in Intersection Over Union (IoU).

The study presented in [18] developed a method called TSegNet, which consisted of 2 stage network. The first network was used for finding a tooth centroid, and the second network was used for tooth segmentation. The study yielded 96.1 % in Dice Similarity Coefficient (DSC) point and 96.9 % in the DSC surface. Another approach using deep learning is studied by Lian et al. [19], that developed a deep learning method called MeshSegNet to segment teeth in 3D data. The study proposed 2 graph-constrained leaning to find 2 locals area with different radii. The study resulted in 98% in DSC.

B. Tooth Landmarking

The study provided in [20] developed automatic tooth landmark recognition. The method began with finding the orientation of the data first to determine the upward side, downward side, left side, right side, forward side, and backward side by using the Principle Component Analysis (PCA). After that, the peak points were calculated with a certain threshold and partitioned each tooth. After that, each tooth found could be identified. It succeeded in determining orientation of the jaw, 79.7% teeth was found, and Modified Huddard Bodemham (MHB) landmark was recognised correctly.

III. The Proposed Method

The proposed method performs a pipeline algorithm that consists of 2 different methods. The first method is mainly used for identifying tooth types, and the second is for finding landmark points.

A. Tooth Segmentation

This study used MeshSegNet method that was developed in [19] using deep learning-based architecture to segment the teeth. It used 3D dental data that is in the form of mesh. It also has 14 labels for each arch, shown in Fig. 1. The algorithm resulted in segmented teeth 3D with decreasing cell number. It helped to reduce the computational process in the next step.

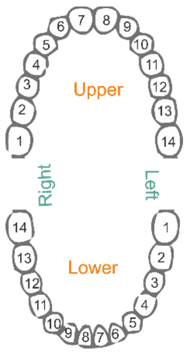

Fig. 1. Tooth Label Used in MeshSegNet

B. Tooth Landmarking

1) Unit Vector Orientation

This study used PCA, the same method used in [20], to obtain the unit vector orientation but with some modifications to determine the sign vector. In that study, because it used raw mesh dental data, it used some statistical method to determine the sign for each direction. However, some cases in that number of faces affected the result. However, this study uses segmented tooth data so the assignment sign process can be done by exploiting the labelled mesh in the data.

The dental mesh data has a unique shape, like the shape of the letter "U", and the points are accumulated on teeth in an upward direction. Therefore, the orientation of the data can be obtained using PCA. PCA works with covariance in all directions. It yields 3-unit vectors representing the largest covariance for the right-left direction, middle-length covariance for the forward-backward direction, and shortest covariance for the upward-downward direction [20]. However, the sign of each unit vector needs to be checked as the unit vector does not have any mean besides covariance.

This study modified the methods used for finding unit vectors. As Fig. 2 presents, the sequence to find the sign begins with finding the forward-backward unit vector sign first, then the upward-downward unit vector sign, and lastly right-left unit vector. But, before doing the calculation, each unit vector has to be inversed by multiplying each element of the unit vector with -1. First, to find the right sign for the forward-backward unit vector, it needs to calculate the mean of the centre of each incisor tooth (1). Then, it needs to do a matrix dot operation with each the forward-backward unit vector and the inverted forward-backward unit vector (2). The unit vector that yields the smallest value from the dot matrix operation becomes the forward-backward unit vector.

The upward-downward sign can be calculated similarly to the forward-backward sign method. But, instead of using the mean of the centre of each incisor tooth, it used the mean of the boundary points of the arch mesh. As the mean value can be changed based on the distribution of the calculated points, it is better to use only half of the number of boundary points to keep the mean value always below the centre of the arch mesh, as Fig. 3 Shows. Using all boundary points has a risk which is the mean value may go upward of the centre of the mesh. The unit vector that yields the biggest value from the dot matrix operation becomes the unit vector for the upward-downward unit vector.

The last is the right-left unit vector whose sign can be determined using the determinant of all unit vectors. Its method uses the same way that study in [20] did. The right-left unit vector uses the inverted value if the determinant value is -1 (3).

$$u_d = \frac{1}{n} * \sum_{i=0}^{n} point_{d_i} \tag{1}$$

where u is mean value, d is index dimension, and n is number of points.

$$dot(A,B) = \sum_{i=0}^{n} (a_i * b_i) \tag{2}$$

where A and B are matrix with the same size, n is number of element in both matrix, i is element index, and a and b are element in both matrix A and B.

$$\det[\hat{e}_{rl}, \hat{e}_{fb}, \hat{e}_{ud}] = \begin{cases} 1\,, using\ not\ inverted \\ -1, using\ inverted \end{cases} \tag{3}$$

where $\hat{e}$ is unit vector, rl is right-left, fb is forward-backward, and ud is upward-downward.

The result of the signed unit vectors can be checked by adding each unit vector and inverted unit vectors with the centre of the mesh points. As Fig. 4 shows, each direction is represented by a point. The red point that is the right-left unit vector represents the right direction, the pink point that is the inverted right-left unit vector represents the left direction, the green point that is the forward-backward unit vector represents the forward direction, the yellow point that is the inverted forward-backward unit vector represents backward direction, the blue point that is the upward-downward unit vector represents the upward direction, and the violet point that is inverted upward-downward unit vector represents the downward unit vector.

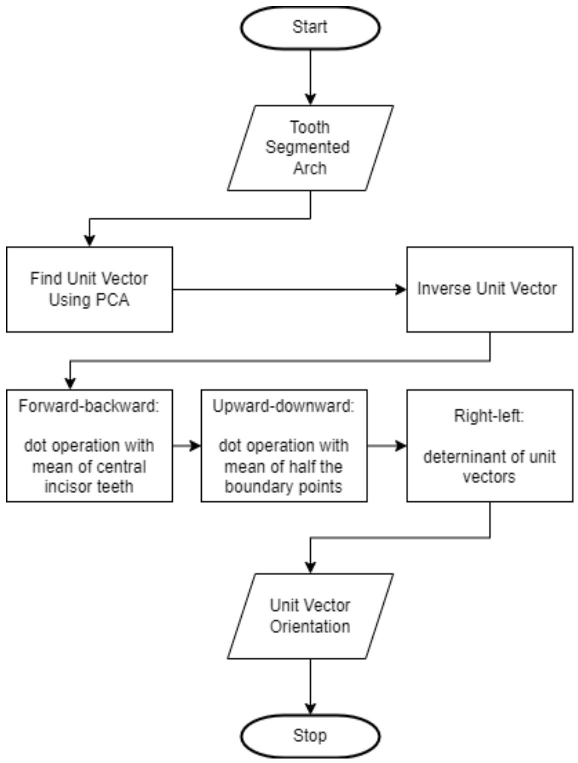

Fig. 2. Orientation Unit Vector Calculation Diagram

2) *Find Landmark Point*

Each tooth has a different form and a different landmark point. For example, the canine tooth may have a mesial point, distal point, buccal point, palatal or lingual point, and cusp point, but the first premolar may have a mesial point, distal point, buccal point, palatal or lingual point, buccal-cusp point, and palatal-cusp or lingual cusp point. For those reasons, the landmark point is calculated individually depending on the type of tooth and landmark. However, each of the calculations has the same steps but the different constant value.

As Fig. 5 shows, it needs an arch mesh orientation unit vector and tooth mesh to find the landmark. First, the tooth mesh resolution is increased with the loop subdivide algorithm (4).

$$new\ cell = \left[\frac{pt_1+pt_2}{2}, \frac{pt_2+pt_3}{2}, \frac{pt_1+pt_3}{2}\right] \qquad (4)$$

where pt is a point in a cell.

After increasing the resolution of the mesh, the points need to be normalized by dividing each point by the mean of the points. Each of the normalized points and the mean of the points need to do a dot operation matrix with each orientation unit vector and inverted orientation unit vector (2). Then, it needs to find the candidate points that meet one or more conditions. For example, landmark pit has a condition that the results of the dot operation matrix from the normalized points with the forward-backward, the inverted forward-backward, the right-left, and the inverted right-left unit vectors are less than the results of the dot operation matrix from the mean of points with the forward-backward, the inverted forward-backward, the right-left, and the inverted right-left unit vectors + 1 respectively. Then finding the final value by calculating the mean of values from the dot operation with a certain constant (5).

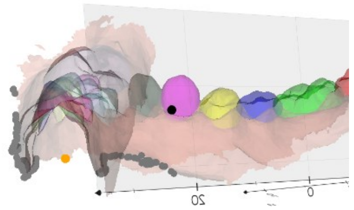

Fig. 3. Boundary Points Selection with black point is the arch's centre, grey points are the chosen boundary points, and orange point is the mean of boundary points.

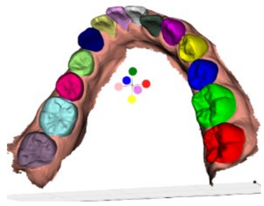

Fig. 4. Orientation Unit Vector Ilustration

$$w_i = \frac{1}{n} * \sum_{i=0}^{n} v_i * c_i \qquad (5)$$

where w is the weighted mean, n is number of the elements, v is value of dot operation matrix, c is a constant for a particular unit vector for a particular landmark which is found using manually trial and error, and i is index of the elements. From those weighted mean values, find the smallest value index. The landmark point is the subdivided tooth mesh points with index from the smallest weighted mean. The illustration of finding landmark point is presented in Fig. 6.

IV. Experimental Result

This study used 3D dental data acquired using an Intra-oral scanner *3Shape* in a dental clinic. In Total, 4 subjects consist of 28 teeth each (14 teeth maxillary and 14 teeth mandibular. The data are in the form of mesh with triangle-shaped cells and have a range of faces between 160000 - 220000. Therefore, after the process of tooth segmentation, the number of faces reduced to 10000 faces.

The experiment in this study was conducted using language programming python 3.9 with library vedo and numpy. The constant used for the weighted mean step is presented in TABLE I. There are no value for a landmark that not exist in certain tooth types that are represented as "-".

The experiment was performed using manually segmented data and deep learning segmented data. Then, the experiment performance was measured using RMSE (7) of the ground truth landmark point and the predicted landmark point for both the upper and lower arch. The RMSE value is calculated for each landmark to show which landmark performs best.

$$Eu_{dist} = \sqrt[2]{(x-\hat{x})^2 + (y-\hat{y})^2 + (z-z)^2} \qquad (6)$$

where Eu_{dist} is Euclidean distance, x , y , and z is x coordinate point of the ground truth point resprectively, and $\hat{x}$, $\hat{y}$, and $\hat{z}$ are x, y, z coordinate point of the predicted point respectively.

$$RMSE = \sqrt[2]{\frac{\sum_{i=0}^{n}\left(Eu_{dist_i}\right)^2}{n}} \qquad (7)$$

TABLE I. TABLE UNIT VECTOR WEIGHT

Arch	**Tooth Label**	**Landmark**				**Arch**	**Tooth Label**	**Landmark**			
		Mesial	***Distal***	***Cusp/ Ridge***	***Pit***			***Mesial***	***Distal***	***Cusp/ Ridge***	***Pit***
Upper	1	RL: 0.2 UD: 0.15 FB: 0.45 Inv RL: 0.2	RL: 0.65 Inv FB: 0.35	UD: 1	Inv UD:1	Lower	1	RL: 0.2 UD: 0.15 FB: 0.45 Inv RL: 0.2	RL: 0.7 Inv FB: 0.3	UD: 1	Inv UD:1
Upper	2	RL: 0.2 UD: 0.15 FB: 0.45 Inv RL: 0.2	RL: 0.65 Inv FB: 0.35	UD: 1	Inv UD:1	Lower	2	RL: 0.2 UD: 0.15 FB: 0.45 Inv RL: 0.2	RL: 0.7 Inv FB: 0.3	UD: 1	Inv UD:1
Upper	3	RL: 0.2 UD: 0.15 FB: 0.45 Inv RL: 0.2	RL: 0.4 UD: 0.1 Inv FB: 0.5	UD: 1	Inv UD:1	Lower	3	RL: 0.2 UD: 0.15 FB: 0.45 Inv RL: 0.2	RL: 0.5 Inv FB: 0.5	UD: 1	Inv UD:1
Upper	4	RL: 0.2 UD: 0.15 FB: 0.45 Inv RL: 0.2	RL: 0.4 UD: 0.1 Inv FB: 0.5	UD: 1	Inv UD:1	Lower	4	RL: 0.2 UD: 0.15 FB: 0.45 Inv RL: 0.2	RL: 0.5 Inv FB: 0.5	UD: 1	Inv UD:1
Upper	5	Inv RL: 0.4 UD: 0.1 FB: 0.5	RL: 0.5 UD: 0.25 Inv FB: 0.25	UD: 0.8 FB: 0.2	-	Lower	5	Inv RL: 0.4 UD: 0.1 FB: 0.5	RL: 0.5 UD: 0.25 Inv FB: 0.25	UD: 0.8 FB: 0.2	-
Upper	6	Inv RL: 0.45 UD: 0.35 FB: 0.2	RL: 0.75 UD: 0.25	UD: 0.8 FB: 0.2	-	Lower	6	Inv RL: 0.45 UD: 0.35 FB: 0.2	RL: 0.75 UD: 0.25	UD: 0.8 FB: 0.2	-
Upper	7	Inv RL: 0.7 UD: 0.4	RL: 0.7 UD: 0.4	UD: 0.8 FB: 0.2	-	Lower	7	Inv RL: 0.7 UD: 0.4	RL: 0.7 UD: 0.4	UD: 0.8 FB: 0.2	-
Upper	8	RL: 0.7 UD: 0.5	Inv RL: 0.7 UD: 0.5	UD: 0.8 FB: 0.2	-	Lower	8	RL: 0.7 UD: 0.5	Inv RL: 0.7 UD: 0.5	UD: 0.8 FB: 0.2	-
Upper	9	RL: 0.45 UD: 0.35 FB: 0.2	Inv RL: 0.75 UD: 0.25	UD: 0.8 FB: 0.2	-	Lower	9	RL: 0.45 UD: 0.35 FB: 0.2	Inv RL: 0.75 UD: 0.25	UD: 0.8 FB: 0.2	-
Upper	10	RL: 0.4 UD: 0.1 FB: 0.5	Inv RL: 0.5 UD: 0.25 Inv FB: 0.25	UD: 0.8 FB: 0.2	-	Lower	10	RL: 0.4 UD: 0.1 FB: 0.5	Inv RL: 0.5 UD: 0.25 Inv FB: 0.25	UD: 0.8 FB: 0.2	-
Upper	11	Inv RL: 0.2 UD: 0.15 FB: 0.45 RL: 0.2	Inv RL: 0.4 UD: 0.1 Inv FB: 0.5	UD: 1	Inv UD:1	Lower	11	Inv RL: 0.2 UD: 0.15 FB: 0.45 RL: 0.2	Inv RL: 0.5 Inv FB: 0.5	UD: 1	Inv UD:1
Upper	12	Inv RL: 0.2 UD: 0.15 FB: 0.45 RL: 0.2	Inv RL: 0.4 UD: 0.1 Inv FB: 0.5	UD: 1	Inv UD:1	Lower	12	Inv RL: 0.2 UD: 0.15 FB: 0.45 RL: 0.2	Inv RL: 0.5 Inv FB: 0.5	UD: 1	Inv UD:1
Upper	13	Inv RL: 0.2 UD: 0.15 FB: 0.45 RL: 0.2	Inv RL: 0.65 Inv FB: 0.35	UD: 1	Inv UD:1	Lower	13	Inv RL: 0.2 UD: 0.15 FB: 0.45 RL: 0.2	Inv RL: 0.7 Inv FB: 0.3	UD: 1	Inv UD:1
Upper	14	Inv RL: 0.2 UD: 0.15 FB: 0.45 RL: 0.2	Inv RL: 0.65 Inv FB: 0.35	UD: 1	Inv UD:1	Lower	14	Inv RL: 0.2 UD: 0.15 FB: 0.45 RL: 0.2	Inv RL: 0.7 Inv FB: 0.3	UD: 1	Inv UD:1

where n is number of points, i is index of the points, and Eu_{dist} is Euclidean distance of the ground truth point and the predicted point (6).

A. Manually Segmented Data

The manually segmented data are clear and neat. They do not have excessive tooth labels. Therefore, the proposed automatic tooth landmarking performance can be seen clearly. The performance of the proposed method using manually segmented data is presented in TABLE II which shows 3.258 in RMSE with both upper and lower arch, 4.318 in RMSE with only upper arch, and 1.746 in RMSE with only lower arch.

The performance of the algorithm for each landmark is shown in

TABLE *III*. It shows that the best landmark is mesial, which has 0.715 in RMSE using the upper arch. Compared to the upper arch's landmark performance, the lower arch's landmark mostly has a better performance.

B. Deep Learning Segmented Data

The experiment used a deep learning algorithm for segmenting tooth yield results, as TABLE II shows. It yields 2.721 in RMSE with both the upper and lower arch, 3.421 in RMSE with only the upper arch, and 1.850 in RMSE with only the lower arch. However, the performance of using deep learning segmented data does not match the given visual

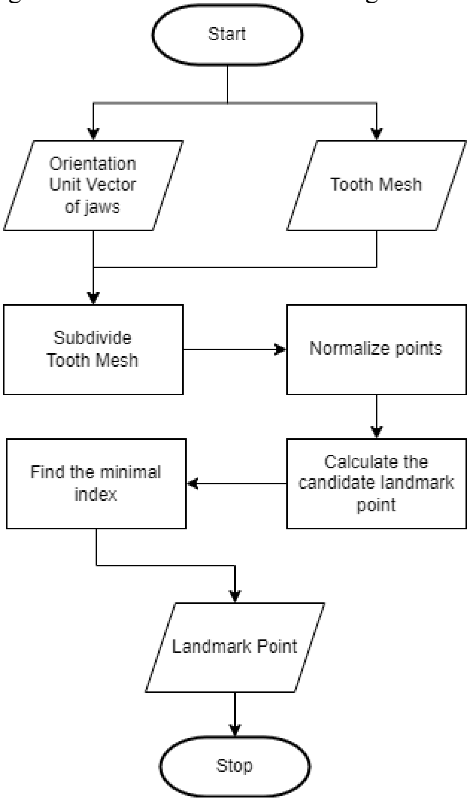

Fig. 5. Tooth Landmarking Diagram

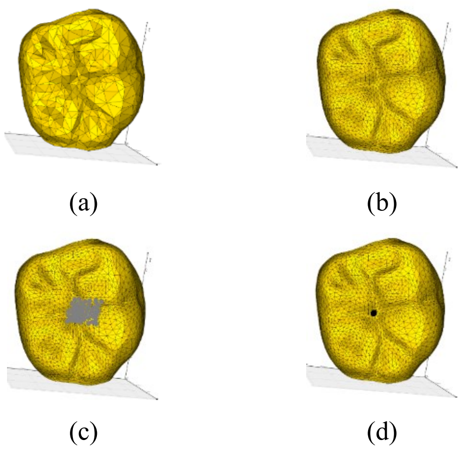

Fig. 6. The Change of the Tooth Mesh in Tooth Landmarking Process. (a) is the Tooth Mesh after Tooth Segmented Process. (b) is the Result of Subdivide Process to Increase Resolution of the Tooth Mesh. (c) is Choosing Candidate Points to be a Landmark. (d) is a Pit Landmark.

TABLE II. TABLE PERFORMANCE ON ARCH

Arch	RMSE	
	Manual	***Deep Learning***
Both Arch	2.734	2.225
Upper Arch	3.488	2.570
Lower Arch	1.746	1.850

TABLE III. TABLE LANDMARK PERFORMANCE ON MANUALLY SEGMENTED DATA

Landmark	Both Arch	Upper Arch	Lower Arch
Mesial	1.094	0.715	1.372
Distal	1.948	1.691	2.175
pit	4.826	4.829	4.824
Cusp/Ridge	7.611	9.106	5.738
cusp buccal/labial	13.142	17.195	7.052
cusp lingual/palatal	16.191	18.241	10.995
cusp buccal/labial mesial	14.111	18.302	7.956
cusp buccal/labial middle	-	-	11.378
cusp buccal/labial distal	14.237	18.406	8.161
cusp lingual/palatal mesial	12.917	18.420	7.202
cusp lingual/palatal distal	13.028	18.499	7.397

TABLE IV. TABLE LANDMARK PERFORMANCE ON DEEP LEARNING SEGMENTED DATA

Landmark	Both Arch	Upper Arch	Lower Arch
Mesial	2.154	2.469	1.792
Distal	3.032	3.498	2.490
pit	6.591	7.785	5.178
Cusp/Ridge	9.278	11.600	6.131
cusp buccal/labial	11.817	15.103	7.531
cusp lingual/palatal	14.140	15.319	11.613
cusp buccal/labial mesial	12.178	14.993	8.476
cusp buccal/labial middle	-	-	12.108
cusp buccal/labial distal	12.420	15.259	8.699
cusp lingual/palatal mesial	11.392	15.436	7.581
cusp lingual/palatal distal	11.596	15.687	7.751

result, as Fig. 7 shows. It presents that the mislabelled cell can reduce the number of recognized teeth. Therefore, it affects the RMSE value.

The performance of the algorithm for each landmark is shown in TABLE IV. It shows that the best landmark is mesial, which has 1.792 RMSE using the lower arch. Compared to the upper arch's landmark performance, the lower arch's landmark mostly has a better performance.

V. CONCLUSION

This study used a pipeline method that consist of deep learning to segment the teeth and weight-based landmarking which is basically transformation operation using the orientation unit vector. The orientation unit vector becomes the essential element, as it determines the upward-downward, forward-backward, and right-left direction of the mesh.

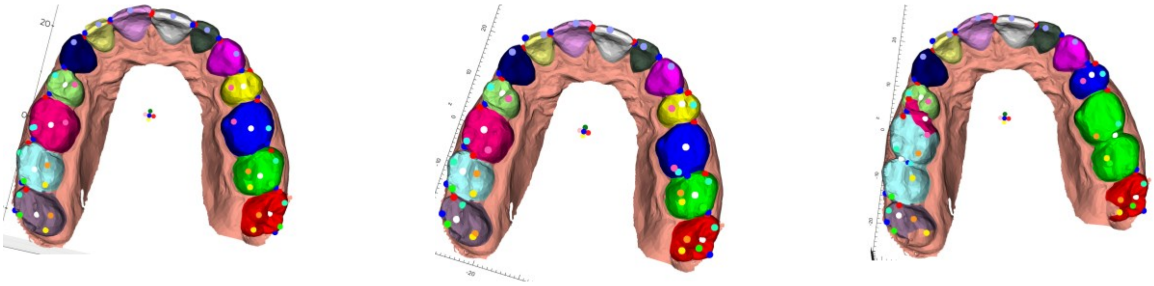

(a) (b) (c)

Fig. 7. (a) Ground Truth (b) Landmark Result with Manually Segmented Data (c) Landmark Result with Deep Learning Segmented Data.

The algorithm successfully detected the landmark points of the tooth. It works well on the mesial and distal points with the RMSE value under 4. For the overall result, the lower arch has a better result in RMSE than the upper one. As the pipeline method, it depends on the first method, deep learning, to label the teeth. Consequently, the automatic landmark labelling can have poor performance if there are many mislabelled teeth.

Many rooms need to be improved, especially in areas where the landmarking process takes the failed labelled teeth. In addition, it needs improvement in posterior teeth landmarking.

ACKNOWLEDGMENT

This research was funded by Lembaga Pengelola Dana Pendidikan (LPDP) under Riset Inovatif-Produktif (RISPRO) Program; the Indonesian Ministry of Education and Culture under Penelitian Terapan Unggulan Perguruan Tinggi (PTUPT) Program; and Institut Teknologi Sepuluh Nopember (ITS) under project scheme of the Publication Writing and IPR Incentive Program (PPHKI).

REFERENCES

[1] S. Sachdev, S. Tantidhnazet, and N. N. Saengfai, "Accuracy of Tooth Movement with In-House Clear Aligners," *J. World Fed. Orthod.*, vol. 10, no. 4, pp. 177–182, 2021.

[2] J. Anh, J.-M. P. Kima, Y.-S. Chun, M. Kim, and M. Kim, "A Comparison of the Precision of Three-dimensional Images Acquired by 2 Digital Intraoral Scanners: Effects of Tooth Irregularity and Scanning Direction," *KOREAN J. Orthod.*, vol. 46, no. 1, pp. 3–12, 2016.

[3] M. A. Saghiri, D. Nath, O. Oguagha, A. M. Saghiri, and S. M. Morgano, "A New Reliable Alternate Method to an Intraoral Scanner (In-vitro Study)," *Phys. Med.*, vol. 12, 2021.

[4] A. Fajar, R. Sarno, C. Fatichah, and A. Fahmi, "Reconstructing and Resizing 3D Images from DICOM Files," *J. King Saud Univ. - Comput. Inf. Sci.*, vol. 34, no. 6, pp. 3517–3526, 2022.

[5] N. Alalwan, A. Abozeid, A. A. Elhabshy, and A. Alzahrani, "Efficient 3D Deep Learning Model for Medical Image Semantic Segmentation," *Alexandria Eng. J.*, vol. 60, no. 1, pp. 1231–1239, 2021.

[6] J. Jorge, G. Ivet, and M. Quinto-sanchez, "Anterior Dental Arch Shape and Human Identification : Kieser Et Al . Method Applied to 2d-3d Dental Models in Mexican Population," *Forensic Sci. Int. Reports*, vol. 2, 2020.

[7] A. Shailendran, T. Weir, E. Freer, and B. Kerr, "Accuracy and Reliability of Tooth Widths and Bolton Ratios Measured by Clincheck Pro," *Am. J. Orthod. Dentofac. Orthop.*, vol. 161, no. 1, pp. 65–73, 2022.

[8] Y. A. Beygelman, R. Khosravi, M. Masoud, D. Turpin, and A. Bollen, "The Influence of Labiolingual and Mesiodistal Anterior Tooth Dimensions on Interarch Relationships: A Modified Anterior Bolton Analysis," *Am. J. Orthod. Dentofac. Orthop.*, vol. 156, no. 6, pp. 727–734, 2019.

[9] A. D. Mongillo, E. A. Araujo, K. B. Kim, and P. F. Foley, "The Effect of 4 First Premolar Extractions on the Posterior Bolton Ratio," *Am. J. Orthod. Dentofac. Orthop.*, vol. 160, no. 6, pp. 825–834, 2021.

[10] M. K. Alam, K. Purman, S. Begum, M. Saifuddin, and M. A. Sikder, "Fallibility of Pont ' s Index in a Bangladeshi Population," *Orthod. Waves*, vol. 73, no. 2, pp. 61–67, 2014.

[11] T. Rastegar-Lari, R. Al-Azemi, L. Thalib, and J. Artun, "Dental Arch Dimensions of Adolescent Kuwaitis with Untreated Ideal Occlusion: Variation and Validity of Proposed Expansion Indexes," *Am. J. Orthod. Dentofac. Orthop.*, vol. 142, no. 5, pp. 635–644, 2012.

[12] M. Revilla-león, J. M. Zeitler, and J. C. Kois, "Digital Maxillomandibular Relationship and Mandibular Motion Recording by Using an Optical Jaw Tracking System to Acquire a Dynamic Virtual Patient," *J. Prosthet. Dent.*, 2022.

[13] L. Lepidi, C. Suriano, H. Wang, S. Granata, T. Joda, and J. Li, "Digital Fixed Complete-arch Rehabilitation: From Virtual Articulator Mounting to Clinical Delivery," *J. Prosthet. Dent.*, vol. 127, no. 3, pp. 398–403, 2022.

[14] M. Palone, G. A. Spedicato, and L. Lombardo, "Analysis of Tooth Anatomy in Adults with Ideal Occlusion: A Preliminary Study," *Am. J. Orthod. Dentofac. Orthop.*, vol. 157, no. 2, pp. 218–227, 2020.

[15] G. Daniele, S. A. Matilde, M. María, R. Villafranca, and A. Martin, "Sex Estimation by Tooth Dimension in a Contemporary Spanish Population," *Forensic Sci. Int.*, vol. 317, 2020.

[16] J. Zhang, C. Li, Q. Song, L. Gao, and Y. Lai, "Automatic 3D Tooth Segmentation Using Convolutional Neural Networks in Harmonic Parameter Space," *Graph. Models*, vol. 109, no. April, p. 101071, 2020.

[17] F. G. Zanjani, D. A. Moin, B. Verheij, F. Claessen, T. Cherici, T. Tan, and P. H. N. D. With, "Deep Learning Approach to Semantic Segmentation in 3D Point Cloud Intra-oral Scans of Teeth," in *Proceedings of Machine Learning Research*, 2019, pp. 557–571.

[18] Z. Cui, C. Li, N. Chen, G. Wei, R. Chen, Y. Zhou, D. Shen, and W. Wang, "TSegNet: An Efficient and Accurate Tooth Segmentation Network on 3D Dental Model," *Med. Image Anal.*, vol. 69, p. 101949, 2021.

[19] C. Lian, L. Wang, T. Wu, F. Wang, P. Yap, C. Ko, and D. Shen, "Deep Multi-Scale Mesh Feature Learning for Automated Labeling of Raw Dental Surfaces From 3D Intraoral Scanners," vol. 39, no. 7, pp. 2440–2450, 2020.

[20] B. Woodsend, E. Koufoudaki, P. A. Mossey, and P. Lin, "Automatic Recognition of Landmarks on Digital Dental Models," *Comput. Biol. Med.*, vol. 137, no. September, 2021.